

MACROSCOPIC MODELING OF TRAFFIC DISPERSION: ISSUES AND PROPOSED SOLUTIONS

Hesham Rakha¹ and Mohamedreza Farzaneh²

Word count: 6,207
Tables and figures: 4,500
Total words: 10,707

ABSTRACT

The paper demonstrates the limitations of the Yu and Van Aerde calibration procedure of the TRANSYT-7F platoon dispersion model, especially for time steps that are greater than 1-second in duration. Subsequently, the paper develops three generalized platoon dispersion models that overcome the limitations of Yu and Van Aerde formulation by explicitly considering the modeling time step in the analytical formulation. The paper validates the proposed models utilizing two datasets. The first dataset includes field data that were gathered in Montréal, Canada, while the second dataset was generated using the INTEGRATION microscopic traffic-simulation software. The results demonstrate that the predicted flow profile using the proposed platoon dispersion models provides a good fit with field-observed and simulated profiles, regardless of the modeling time step that is considered, while the results also demonstrate the deficiencies of Yu and Van Aerde formulation, especially for time steps that are greater than 1-second in duration.

INTRODUCTION

Vehicles departing from a queue at a traffic signal typically travel in a platoon that disperses as vehicles travel further downstream. In part, the platoon dispersion is caused by differences in drivers' desired speeds, and mostly as a result of vehicle interaction with other vehicles entering and exiting the roadway, which is commonly known as the roadway-side friction. Platoon dispersion models attempt to simulate the dispersion of traffic as it travels along a roadway by attempting to estimate vehicle arrivals at downstream locations based on an upstream vehicle departure profile and a desired traffic-stream speed.

The most widely used platoon dispersion model is Robertson's (1969) model. This model has become a virtual universal standard platoon dispersion model and has been implemented in various traffic-simulation software, including TRANSYT (Robertson, 1986), SCOOT (Hunt *et al.*, 1989), SATURN (Hall *et al.*, 1980), and TRAFLO (Lieberman *et al.*, 1980). A successful application of Robertson's platoon dispersion model requires an appropriate calibration of the model's parameters. Specifically, Guebert and Sparks (1989) showed that the accurate calibration of the Robertson platoon dispersion model parameters was critical in developing effective and efficient traffic signal timing plans. Despite the significant impact the platoon dispersion parameters have on the signal timings that are estimated by the TRANSYT-7F software, the software manual does not provide an analytical framework for the calibration

¹ Associate Professor, Charles Via Jr. Department of Civil and Environmental Engineering, 3500 Transportation Research Plaza (0536), Blacksburg VA 24061. E-mail: hrakha@vt.edu.

² Graduate Research Assistant, Charles Via Jr. Department of Civil and Environmental Engineering, 3500 Transportation Research Plaza (0536), Blacksburg VA 24061.

of the platoon dispersion model parameters. The state-of-practice has been the use of a goodness-of-fit approach to calibrate the model parameters. Alternatively, Yu and Van Aerde (2000) developed an analytical framework for calibrating the platoon dispersion model parameters using a statistical analysis of link travel-time distribution. Specifically, Yu and Van Aerde proposed a set of formulas to calibrate the parameters of Robertson's platoon dispersion model based on the average travel time and the standard deviation of the travel time, as will be described later in further detail.

Robertson's platoon dispersion model, which is also known as the TRANSYT platoon dispersion model, is naturally a discrete time model that calculates the estimated flow downstream by dividing the departure profile into time steps. This paper demonstrates that the accuracy of the predicted downstream flow profile using the parameters derived by Yu and Van Aerde is highly dependent on the duration of the modeling time step. Specifically, as the length of the time step increases, the accuracy of the predicted downstream profile decreases.

The objective of this paper is to not only demonstrate the limitations of the Yu and Van Aerde calibration method but to develop a modified formulation that addresses these limitations. The proposed models are derived using a generalized parametric second-by-second platoon dispersion analysis of the basic TRANSYT platoon dispersion model. The proposed models are then validated using two data sets: namely, a field and simulation dataset.

STATE-OF-PRACTICE TRAFFIC DISPERSION FORMULATIONS

This section describes the state-of-practice and state-of-art platoon dispersion models. The most common of these platoon dispersion models are Pacey's diffusion model and Robertson's recursive model, which are described below. Enhancements to the Robertson's platoon dispersion model are also described.

Pacey's Formulation: Diffusion Theory

In an unpublished research note at the Road Research Laboratory, Pacey (1956) presented a purely kinematical platoon dispersion model that is remarkably simple. Specifically, Pacey claimed that the only changes in the shape of a platoon of vehicles released from a signalized approach arise from differences in vehicle speeds within the platoon assuming that any vehicle proceeds with the same speed irrespective of the number or distribution of vehicles on the road, and that vehicles are able to pass slow-moving vehicles in order to maintain their desired speed.

In his derivation, Pacey adopted a normal distribution as the distribution of vehicle speeds within a platoon. Seddon (1972a) showed that using the distribution of vehicle velocities $f(v).dv$, it is possible to obtain the distribution of vehicle travel times $g(T).dT$ between any two observation points. Using the distribution of travel times, Seddon demonstrated that the downstream flow within a time interval can be estimated using the following discrete form:

$$q'_t = \sum_{i=T}^{\infty} g(i-T).q_{t-i} \quad [1]$$

Where:

q'_t : Arrival flow at the downstream intersection at time t (veh/h);

q_t : Departure flow at the upstream intersection at time t (veh/h);

T : Minimum travel time between two observation points (units of time steps); and

$g(i-T)$: Probability of a travel time of $(i-T)$ time steps.

To calibrate Pacey's model, one needs two parameters: average speed V and standard deviation, σ_v , of the speed of the vehicles traveling on the link. These two parameters can be obtained from field measurement or by using a best fit method varying V and σ_v to minimize the sum of squares of the differences of observed and predicted flow in each interval.

Robertson's Recursive Formulation

The most commonly used macroscopic approach to the mathematical modeling of the platoon dispersion process is the Robertson platoon dispersion model, which was developed for the TRANSYT software (Robertson, 1969). The Robertson platoon dispersion model has become virtually the universal standard and has been incorporated in a number of softwares, including the Split Cycle Offset Optimization Tool (SCOOT) (Hunt *et al.*, 1989), SATURN (Hall *et al.*, 1980), and TRAFLO (Lieberman *et al.*, 1980).

The basic Robertson recursive platoon dispersion model takes the following mathematical form:

$$q'_t = F.q_{t-T} + (1-F).q'_{t-\Delta t} \quad [2]$$

$$F = \frac{1}{1 + \alpha.\beta.T_a} \quad [3]$$

Where:

- Δt : time step duration, measured in the time intervals used for q'_t and q_t ;
- T : minimum travel time on the roadway in units of time steps, equal to $\beta.T_a$;
- α : dimensionless platoon dispersion factor;
- β : dimensionless travel-time factor;
- F : smoothing factor, and
- T_a : mean roadway travel time, measured in units of time steps.

Equation 2 is applied by dividing the departure profile from an upstream traffic signal into a number of time steps. For example, the TRANSYT-7F model divides the cyclic profile into a total of 60 time steps that typically range in duration between 1 to 3 seconds. The arrival profile at the downstream signalized intersection at instant t is then computed using Equation 1 as the weighted combination of the downstream flow one time step earlier ($q'_{t-\Delta t}$) and the upstream departure flow T seconds earlier (q_{t-T}).

Seddon (1972b) rewrote Equation 1 in the form

$$q'_t = \sum_{i=T}^{\infty} F.(1-F)^{i-T}.q_{t-i}, \quad [4]$$

which is a special case of the general form of Equation 1.

Equation 4 demonstrates that the downstream traffic flow that is computed using the Robertson platoon dispersion model follows a shifted geometric distribution, as demonstrated in Figure 1. The geometric distribution gives the probability that a vehicle passing the upstream point in the $(t-i)^{\text{th}}$ interval is observed downstream in the i^{th} interval. Robertson (1969) assumed the travel-time factor (β) to be fixed at a value of 0.8, and it has since been fixed at 0.8, while the platoon dispersion factor (α) was allowed to vary between 0.2 and 0.5, depending on the level of friction along the roadway. The TRANSYT-7F User's Guide recommends that the platoon dispersion factor α vary depending on the site-specific geometric and traffic conditions. The typical procedure for calibrating the platoon dispersion factor is to select the platoon dispersion factor that minimizes the sum-of-squared error between field-observed and estimated downstream flow profiles for a given upstream flow profile.

Yu and Van Aerde Calibration Procedure

A successful application of Robertson's platoon dispersion model relies on the appropriate calibration of the model parameters. Specifically, studies have shown that platoon dispersion parameters are site-specific and a function of roadway grades, curvature, parking, opposing flow interference, traffic volume, and other sources of impedance. Furthermore, these studies have demonstrated that the use of the TRANSYT-7F default platoon dispersion parameters results in significant errors in the modeling of platoon movement along roadways and thus results in inefficient traffic signal timings.

Yu and Van Aerde (2000) not only demonstrated that the travel-time factor (β) is dependent of the platoon dispersion factor (α) but also developed a method for calibrating the Robertson platoon dispersion factors (α and β) directly from the statistical properties of the travel-time experiences of individual vehicles. Specifically, the authors used the basic properties of the geometric distribution of Equation 4 to derive the following three equations for calibrating the parameters of the Robertson platoon dispersion model. A detailed description of how these equations were derived is provided in appendix A.

$$\alpha = \frac{1 - \beta}{\beta} \quad [5]$$

$$\beta = \frac{2T_a + 1 - \sqrt{1 + 4\sigma^2}}{2T_a} \quad [6]$$

$$F = \frac{\sqrt{1 + 4\sigma^2} - 1}{2\sigma^2} \quad [7]$$

Where:

σ : standard deviation of link travel times (s), and

T_a : mean roadway travel time (s).

Equation 5 demonstrates that the value of the travel-time factor β is dependent on the value of the platoon dispersion factor α , as opposed to a fixed value of 0.8, which is currently implemented in the TRANSYT-7F software. Equation 6 shows that the value of the travel-time factor can be calibrated from the expected (T_a) roadway travel time and the travel-time variance (σ^2).

The Yu and Van Aerde calibration procedure demonstrates that the Robertson platoon dispersion model requires the calibration of a single parameter (α) given that the travel-time shift factor (β) is dependent on the value of the smoothing factor. Incorporating Equation 5 into Equation 3, we derive

$$F = \frac{1}{1 + (1 - \beta)T_a} = \frac{1 + \alpha}{1 + \alpha(1 + T_a)} \quad [8]$$

Equation 8 demonstrates that the smoothing factor (F) can be expressed as a function of either β or α . Using α and β values that are not consistent with Equation 5 results in an output average travel time that is inconsistent with the desired input average travel time.

Effect of Travel Time Distribution on Platoon Dispersion

As demonstrated by Seddon (1972b) the state-of-practice Robertson platoon dispersion model is a specific case of the more general form that was presented earlier in Equation 1. Specifically, in the case of the Robertson platoon dispersion model, the link travel time distribution is assumed to follow a shifted geometric distribution.

Yu and Van Aerde (1995) studied the effect of the underlying travel time distribution on the predicted downstream cyclic flow profile. Specifically, the authors considered a normal distribution of vehicle speeds, a shifted geometric distribution of trip travel times, and a normal distribution of travel times. The authors demonstrated that although the fundamental probability distribution for the predicted downstream distribution was significantly different considering a single upstream link flow pulse, the dispersion of a cyclic flow profile produced minimal differences in the estimated downstream flow profiles. Consequently, it was concluded that the particular shape of the statistical distribution that is used to represent the dispersion modeling has a marginal effect on the predicted downstream flow profile. For example, Figure 2 depicts the resulting downstream flow profile considering different statistical probability functions in the dispersion model of Equation 1. Table 1 lists the implemented models and their respective input parameters considering an equal mean and standard deviation of travel time. The figure clearly demonstrates that the differences in the predicted downstream flow profiles are marginal, as was demonstrated earlier by Yu and Van Aerde (1995).

It should be noted that Equations 5 and 6 demonstrate that the roadway platoon dispersion factors α and β are dependent and vary as a function of the roadway travel time mean and standard deviation. Consequently, the calibration procedures that were developed by Yu and Van Aerde are a significant contribution to the state-of-practice procedures in modeling traffic dispersion.

Example Application of State-of-Practice Formulations

Seddon (1972b) demonstrated that the basic assumption of the Robertson platoon dispersion model is that the traffic-stream travel time follows a shifted geometric distribution. It should be noted, however, that the shifted geometric distribution is a discrete probability function that ensures that roadway travel times exceed a minimum roadway-specific travel time (T). We demonstrate in this paper that because Yu and Van Aerde considered travel times in units of seconds in the derivation of their calibration procedure, the procedure is only valid when a 1-second time step is considered. Consequently, the cyclic flow profile prediction error increases as the duration of the modeling time step increases.

In an attempt to demonstrate the effect of the modeling time step on the downstream flow profile prediction error, the dispersion of an upstream flow profile was modeled considering different time step durations, as demonstrated in Figure 3. Specifically, the downstream flow profile, as computed considering different time step durations, was compared to predicted flow profiles considering a 1-second step. The figure clearly demonstrates that the predicted downstream flow profile changes as the modeling step size increases and that the prediction error increases with an increase in the modeling step size. Specifically, as the step size increases, the cyclic profile dispersion increases. For example, the utilization of a 1-second step size produces the highest maximum flow and the smallest dispersion, and as the step size increases, the maximum flow decreases and is dispersed more. The cyclic profile prediction error, which was computed as the difference in predicted flow profile each second, increases as the modeling step size increases.

The example illustration demonstrates the inherent shortcoming of the platoon dispersion formulation that was proposed by Yu and Van Aerde (1995). Specifically, the dispersion modeling accuracy decreases as a function of modeling step size.

PROPOSED TRAFFIC DISPERSION MODEL ENHANCEMENTS

The shortcomings of the Yu and Van Aerde calibration procedure arise from a lack of consistency in units of several parameters within the formulation. Specifically, the unit of time used in calculating the α , β and F parameters are in seconds while the units of time for the remainder parameters are in units of time interval durations. Consequently, the model estimates travel time probabilities that are inconsistent

with the desired travel times. The following sections describe three proposed formulations to overcome the identified shortcomings.

First Approach: Second-by-Second Parametric Analysis

A simple approach to overcome the shortcoming of the Yu and Van Aerde method for calibrating the Robertson platoon dispersion model in modeling time steps that are greater than 1-second in duration is to disaggregate the upstream flow profile considering 1-second time steps. Subsequently, the dispersion of the disaggregated upstream flow profile can be performed utilizing Equation 4 to predict a disaggregated downstream flow profile using the parameters derived from Equations 5 through 7. Finally, the downstream disaggregated flow profile can then be aggregated to the desired time step to estimate the aggregated downstream flow profile. In summary, the use of a second-by-second numerical solution to Equation 4 is derived analytically to develop a generalized formulation, as will be presented in this section.

The proposed approach is initially described and derived for a step size of 3 seconds for illustration purposes and is then generalized for any step size. Figure 4 illustrates the second-by-second parametric analysis for a 3-second time-step example. Considering a single 3-second flow rate (q) departing from an upstream traffic signal, the flow can be disaggregated into three equal 1-second flow profiles, each of flow rate q . Subsequently, the downstream flow profile for each of the three one-second flow pulses can be estimated using Equation 4, as illustrated in Figure 4. Subsequently, the disaggregated flow profile can be aggregated to generate the desired 3-second flow profile. The first 1-second upstream flow rate of q results in flows q'_1 , q'_2 , and q'_3 during the first 3-second time interval of the downstream profile. Similarly, the second 1-second upstream flow pulse, which is temporally shifted by 1 second, produces flows q'_1 and q'_2 during the first 3-second time interval at the downstream location. Finally, the third 1-second flow rate of q results in a single flow rate of q'_1 at the downstream location during the first 3-second interval. Aggregating the downstream flow profile considering a 3-second time step produces a flow rate of q'_{t1} , as

$$q'_{t1} = \frac{1}{3} \cdot [(q'_1 + q'_2 + q'_3) + (q'_1 + q'_2) + (q'_1)] = q'_1 + \frac{2}{3}q'_2 + \frac{1}{3}q'_3. \quad [9]$$

Substituting the downstream flows that are derived using Equation 4 into Equation 9, the aggregated first 3-second flow rate can be computed as

$$q'_{t1} = \left[(1-F)^0 + \frac{2}{3}(1-F)^1 + \frac{1}{3}(1-F)^2 \right] \cdot F \cdot q. \quad [10]$$

Applying the same approach for the second and third time step, we obtain

$$\begin{aligned} q'_{t2} &= \frac{1}{3} \cdot [(q'_4 + q'_5 + q'_6) + (q'_3 + q'_4 + q'_5) + (q'_2 + q'_3 + q'_4)] = \frac{1}{3}q'_2 + \frac{2}{3}q'_3 + q'_4 + \frac{2}{3}q'_5 + \frac{1}{3}q'_6 \\ &= \left[\frac{1}{3}(1-F)^1 + \frac{2}{3}(1-F)^2 + (1-F)^3 + \frac{2}{3}(1-F)^4 + \frac{1}{3}(1-F)^6 \right] \cdot F \cdot q, \end{aligned} \quad [11]$$

and

$$\begin{aligned} q'_{t3} &= \frac{1}{3} \cdot [(q'_7 + q'_8 + q'_9) + (q'_6 + q'_7 + q'_8) + (q'_5 + q'_6 + q'_7)] = \frac{1}{3}q'_5 + \frac{2}{3}q'_6 + q'_7 + \frac{2}{3}q'_8 + \frac{1}{3}q'_9 \\ &= \left[\frac{1}{3}(1-F)^4 + \frac{2}{3}(1-F)^5 + (1-F)^6 + \frac{2}{3}(1-F)^7 + \frac{1}{3}(1-F)^8 \right] \cdot F \cdot q. \end{aligned} \quad [12]$$

Generalizing Equations 10, 11, and 12 for all time intervals, the aggregated 3-second downstream flow profile can be computed, as follows:

$$q'_t = \sum_{i=0}^{\infty} F \cdot q_{t-(T+3i)} \times \sum_{k=\max[3i-2,0]}^{3i-2} \left((1-F)^k \cdot \frac{3-|3i-k|}{3} \right) \quad [13]$$

Where:

q'_t : aggregated 3-second downstream flow rate at time interval t^1 (veh/h);

q_t : aggregated 3-second upstream flow rate at time interval t (veh/h) ; and

F : smoothing factor calculated using Equation 7.

Generalizing Equation 12 for any bin size, the final formulation is derived as

$$q'_t = \sum_{i=0}^{\infty} F \cdot q_{t-(T+i \cdot n)} \times \sum_{k=\max[i \cdot n-(n-1),0]}^{i \cdot n+(n-1)} \left((1-F)^k \cdot \frac{n-|i \cdot n-k|}{n} \right). \quad [14]$$

Where:

q'_t : aggregated n-second downstream flow rate at time interval t (veh/h);

n : time step duration (s) ; and

q_t : aggregated n-second upstream flow rate at time interval t (veh/h).

T was defined earlier in the Robertson formulation, while the parameters α , β , and F are calibrated using Equations 5, 6 and 7, respectively. Equation 14 demonstrates that the aggregated downstream traffic flow depends on the size of the time interval. In fact, Equation 14 is a generalized form of the geometric distribution that ensures consistency across different time interval sizes, since it ensures consistency in the time units across the various model parameters.

Second Approach: Second-by-Second Parametric Analysis Ignoring Differences in Dispersion within a Time Interval

While the approach that was described earlier generalizes the Yu and Van Aerde calibration procedure for time intervals greater than 1 second in duration, it is computationally intensive and complex. The model complexity arises from the fact that the model disaggregates a flow profile to its lowest temporal resolution (time interval of 1 second) prior to dispersing the flow profile and subsequently re-aggregates the downstream flow profile. A simpler approach can be derived by performing a second-by-second parametric analysis; however, in this case the dispersion of each 1-second flow pulse within the modeling time interval is assumed to be identical.

In this approach, it is assumed that every 1-second upstream flow pulse within the time interval $(i-T)$ produces the same flow in the i^{th} time interval of the downstream profile. In other words, all 1-second upstream flows in interval $(i-T)$ have the same downstream profile as the downstream flow shown in Figure 4a. Performing the same analysis that was done in the previous section we can calculate the rate of q'_{t1} , as follows:

$$q'_{t1} = \frac{1}{3} \cdot [(q'_1 + q'_2 + q'_3) + (q'_1 + q'_2 + q'_3) + (q'_1 + q'_2 + q'_3)] = q'_1 + q'_2 + q'_3 \quad [15]$$

¹ t represents the mid-point of the time interval.

Substituting the downstream flows using Equation 4 in Equation 15, the aggregated first 3-second flow rate can be computed as:

$$q'_{t_1} = [(1-F)^0 + (1-F)^1 + (1-F)^2] \cdot F \cdot q. \quad [16]$$

Applying the same approach for the second and third time steps we obtain

$$\begin{aligned} q'_{t_2} &= \frac{1}{3} \cdot [(q'_4 + q'_5 + q'_6) + (q'_4 + q'_5 + q'_6) + (q'_4 + q'_5 + q'_6)] = q'_4 + q'_5 + q'_6 \\ &= [(1-F)^3 + (1-F)^4 + (1-F)^6] \cdot F \cdot q, \end{aligned} \quad [17]$$

and

$$\begin{aligned} q'_{t_3} &= \frac{1}{3} \cdot [(q'_7 + q'_8 + q'_9) + (q'_7 + q'_8 + q'_9) + (q'_7 + q'_8 + q'_9)] = q'_7 + q'_8 + q'_9 \\ &= [(1-F)^6 + (1-F)^7 + (1-F)^8] \cdot F \cdot q. \end{aligned} \quad [18]$$

Generalizing Equations 16, 17, and 18 for a 3-second aggregation interval we derive

$$q'_t = \sum_{i=0}^{\infty} F \cdot q_{t-(T+3i)} \times \sum_{k=3i+1}^{3i+3} (1-F)^{k-1}. \quad [19]$$

Where:

- q'_t : aggregated 3-second downstream flow rate at time interval t ¹ (veh/h);
- q_t : aggregated 3-second upstream flow rate at time interval t (veh/h); and
- F : smoothing factor calculated using Equation 7.

Generalizing Equation 19 for any bin size, the final formulation can be written as

$$q'_t = \sum_{i=0}^{\infty} F \cdot q_{t-(T+i \cdot n)} \times \sum_{k=i \cdot n+1}^{i \cdot n+n} (1-F)^{k-1}. \quad [20]$$

Where:

- q'_t : aggregated n -second downstream flow rate at time interval t (veh/h);
- n : time step duration (s); and
- q_t : aggregated n -second upstream flow rate at time interval t (veh/h).

Comparing Equation 20 to Equation 4, it is evident that Equation 20 is identical to Equation 4 and therefore can be recast as

$$\sum_{k=i \cdot n+1}^{i \cdot n+n} F \cdot (1-F)^{k-1} = g(i-T) = GCDF(i \cdot n+n) - GCDF(i \cdot n). \quad [21]$$

Where:

- GCDF() : Cumulative probability of shifted geometric distribution.

Equation 20 demonstrates that the aggregated downstream traffic flow profile can be estimated using the corresponding geometric distribution while ensuring consistency between the geometric distribution and

¹ t represents the mid-point of the time interval.

cyclic flow profile. As was mentioned earlier, incompatibilities in bin boundaries are the main reason for the shortcomings of the Yu and Van Aerde calibration procedure for time steps greater than 1-second in duration. Like Equation 14, Equation 20 ensures consistency between the statistical dispersion distribution and the temporal time steps of the upstream cyclic profile; however, the accuracy of the dispersion model is less than the earlier formulation (Equation 14) because traffic dispersion is assumed to be identical for all 1-second sub-intervals within the modeling time interval, as will be discussed in the following section.

Third Approach: Equivalent Dispersion Distribution

Both of the above approaches consider a geometric distribution of 1-second step size and generalize it to be consistent with the desired non-1-second analysis time interval. Another approach to achieve consistency across the various step sizes is to find a set of β , F and α values for the desired step size that approximates 1-second step size geometric distribution. To obtain this new set of parameters, we can rewrite Equations 5, 6, and 7 as

$$\alpha_n = \frac{1 - \beta_n}{\beta_n}, \quad [22]$$

$$\beta_n = \frac{2T'_a + 1 - \sqrt{1 + 4\sigma'^2}}{2T'_a}, \text{ and} \quad [23]$$

$$F_n = \frac{\sqrt{1 + 4\sigma'^2} - 1}{2\sigma'^2}. \quad [24]$$

Where:

β_n , F_n and α_n : model parameters for step size of n seconds,

σ' : standard deviation of link travel times (in units of time steps) equals to σ/n , and

T'_a : mean roadway travel time (in units of time steps) equals to T_a/n .

Substituting σ' and T'_a for σ and T_a in Equations 23 and 24 we derive

$$\beta_n = \frac{2T_a + n - \sqrt{n^2 + 4\sigma^2}}{2T_a}, \text{ and} \quad [25]$$

$$F_n = n \cdot \frac{\sqrt{n^2 + 4\sigma^2} - n}{2\sigma^2}. \quad [26]$$

Where:

σ : standard deviation of link travel times (s), and

T_a : mean roadway travel time (s).

Equations 25 and 26 demonstrate that the values of β , F and α are dependent on the size of the time interval. In addition it can be observed that the relationship between β , F and α is as follows;

$$F_n = \frac{1}{1 + \alpha_n \cdot \beta_n \cdot T'_a} = \frac{n}{n + (1 - \beta_n)T_a} \quad [27]$$

Equations 26 and 27 demonstrate that the smoothing factor (F) is not dimensionless as is suggested by Yu and Van Aerde (2000); instead its units are the inverse of time.

Numerical Example Application of Proposed Formulations

In an attempt to demonstrate how the proposed models can be applied, a simple example illustration is presented in which an upstream flow profile is considered and each of the proposed models is utilized to predict the downstream flow profile for the initial 8 seconds. The assumed upstream flow profile contains two time intervals of 4-second duration. The first interval, from $t = 0\text{s}$ to $t = 4\text{s}$, has a flow rate of 2000 veh/h/lane and the second interval, from $t = 4\text{s}$ to $t = 8\text{s}$, has a flow rate of 1000 veh/h/lane. The average travel time between the upstream and downstream points (T_a) is 40s with a travel time standard deviation of 8.46s, which corresponds to a $\beta = 0.8$, $F = 0.111$ and $\alpha = 0.25$ based on Equations 5 through 7.

The step-by-step calculation of the proposed models is tabulated in Tables 2 through 4 for illustration purposes. Calculations are performed to estimate two consecutive 4-s intervals of the downstream flow profile (k ranges from 1 to 8 for models 1 and 2). The first column of each table refers to the time stamp at the mid-point of the downstream interval (downstream interval index). The second column lists the values of i for which the term in the summation returns non-zero values. It should be noted that a maximum of two values of i are available for each interval because we are only predicting the flow profile for the initial two intervals. Column 4 provides the upstream flow rate during the considered time interval. Columns 5 through 12 of Tables 2 and 3 provide the calculated w_k values. It should be noted that in the case of the first and second models (Table 2 and 3) the upstream flow rate of 2000 veh/h/lane contributes to flows during the first and second downstream time steps (34s and 38s, respectively), while the second pulse of 1000 veh/h/lane only contributes to the second time step. Column 13 of Tables 2 and 3 provides the summation of w_k values, which is the probability that an upstream pulse results in a downstream pulse. The actual number of vehicle arrivals during a time step is then computed by multiplying the probability by the upstream flow rate. The contributions of the different upstream time steps are then summed up to compute the downstream flow profile, as demonstrated in the last column of Tables 2 and 3. In the case of the third proposed model (Table 4) the w_k factors are not calculated because the model computes the equivalent smoothing factor that reflects the modeling step size as opposed to disaggregating the two steps into the eight 1-second steps, as is the case of the first two models. The final column of each table computes the total flow rate in each of the 4-sec downstream intervals. A comparison of the results demonstrates that apart from the first time step, all approaches produce very similar downstream flow estimates.

MODEL VALIDATION

This section describes the validation effort of the proposed models. Specifically, two datasets are utilized for validation purposes. These datasets include a field dataset that was gathered in Montréal, Canada, by Manar (1994) and a dataset that was generated as part of this study using the INTEGRATION microscopic traffic simulation software.

Montréal Field Data

The field dataset that is utilized for validation purposes was gathered by Manar (1994) in Montréal, Canada. The test site is a section of Papineau Ave. between Rue De Louvein and Emile Journault Ave., Montréal, Canada. Papineau Ave. is a 6-lane arterial roadway (3-lanes per direction of travel). Three video cameras were installed in the field to observe and record the progression of platoons along the roadway. The video cameras were set up at locations A, B, and C, as illustrated in Figure 5.

Using the video data, the number of vehicles within 2-second intervals was recorded at the three locations. Because the mean and variance of individual travel times were not available, these parameters were estimated by minimizing the sum of the squared error between the observed and

estimated 1-second flow profiles by varying the T_a and σ parameters and then calculating the β , F and α parameters using Equations 22, 23, and 24.

The upstream flow profile (at point A) was then aggregated to reflect time steps of 4 and 6 seconds in addition to the base case of 2 seconds, as illustrated in Figure 6. The downstream flow profile was estimated at locations B and C using the proposed dispersion models, the Robertson dispersion model (calibrating α and β parameters independently), by calibrating the α and β parameters using the Yu and Van Aerde procedures, and by calibrating the α parameter using a best-fit approach (Robertson) and setting the β parameter at a value of 0.8, as implemented in the TRANSYT-7F software.

Figure 7 demonstrates how the estimated downstream flow profiles compared to the field-observed profiles for the three time-step configurations. The figure clearly demonstrates a deterioration in the accuracy of the estimated downstream flow profile when the Yu and Van Aerde formulation is applied. Alternatively, the proposed models are able to estimate the downstream profile with a level of accuracy that does not deteriorate as the modeling time step increases, as demonstrated in Figure 8. Specifically, Figure 8 clearly depicts an increase in the Yu and Van Aerde model prediction error as the analysis step-size increases. This increase in the error can be attributed to the fact that the computed error is composed of two errors: a prediction error and a variability error. The prediction error results from errors in predicting the downstream profile, while the variability error results from variability in individual vehicle travel times along the study section. As the modeling time step increases, the variability error decreases - given that more vehicles are considered within each time step. Although the variability error decreases as the time step increases in the case of the Yu and Van Aerde formulation, the prediction error increases substantially. This results in an overall increase in the computed error. In the case of the proposed models, however, the total error decreases slightly as the time step increases because the prediction error remains virtually constant, while the random error decreases as the time step increases. The total error of the Robertson formulation with a fixed β remains almost constant for the different time steps and in fact tends to increase as time steps increase.

Amongst all the models that were examined, excluding the Yu and Van Aerde formulation, the proposed model-1 produces the least error compared to all other cases, which is expected since it utilizes a higher level of resolution (1-second analysis). The proposed model-3 produces the second highest accuracy and the Robertson formulation and proposed model-2 have the highest error. The results demonstrate the level of consistency that each model is able to maintain for different time step values. Although the Robertson formulation with fixed value of β and proposed model-2 show approximately the same level of prediction error, it should be noted that the ideal value of α was utilized. It is customary for TRANSYT-7F users to utilize the default platoon dispersion factor of 0.35. Furthermore, the TRANSYT-7F model considers a single network-wide platoon dispersion factor. Consequently, from a practical standpoint the model error is expected to increase.

Microscopic Simulation Analysis

An additional validation effort was conducted using the INTEGRATION traffic-simulation model. This effort serves two purposes. First, it demonstrates the validity of the INTEGRATION software for the modeling of platoon dispersion behavior. Such a validation is critical in order to utilize the INTEGRATION software to construct a database of traffic dispersion behavior. The use of simulation is critical to conduct a detailed sensitivity analysis of various traffic-stream factors on traffic dispersion. Second, this validation effort further validates the proposed analytical formulations.

The simulation was conducted using the INTEGRATION traffic-simulation and assignment software, which was developed to model the interaction of freeways and surface streets, simulation and traffic assignments, static and dynamic controls, and routing in an integrated fashion (Van Aerde, 1985; Van Aerde and Yagar, 1988a and b; Rakha and Ahn, In press). The model represents the movement of individual vehicles in a time-stepping fashion, based on a steady-state car-following relationship for each

link. It should be mentioned that INTEGRATION is a fully microscopic simulation model; however, the microscopic rules used in it have been carefully calibrated in order to capture the most important macroscopic traffic characteristics. A detailed description of the model calibration procedures is beyond the scope of this paper but is described in detail in the literature (Van Aerde and Rakha, 1995; Rakha and Crowther, 2003).

The validation effort considered a configuration similar to the Montréal field data. Specifically, vehicles departed from an upstream traffic signal and were monitored as they traveled downstream along a three-lane roadway. Specifically, three loop detectors were placed on the roadway. The first loop detector was located immediately upstream from the upstream signalized intersection, while the other two detectors were located 200 and 300 meters downstream of the traffic signal, respectively. The loop detectors gathered data at 2-second intervals as was done in the Montréal study. Figure 9 depicts the network layout, while Table 6 summarizes the roadway and network characteristics that were simulated.

The simulation run continued for 600 seconds and consisted of six distinct platoons of vehicles that departed from the upstream traffic signal. All the vehicles were passenger cars. Travel-time variability was captured by modeling randomness in vehicle speeds as a random variable that followed a normal distribution with a 10 percent Coefficient of Variation (CV) about the mean steady-state desired speed. All simulated vehicles were set as probes to record their individual travel times in computing the expected and travel-time variance for the calibration of the α and β parameters, as was described earlier. A summary of the calibrated parameters is provided in Table 7.

Two time steps were considered in the analysis: namely, a 2 and 6-second time step. The simulated and estimated downstream flow profiles were computed using the proposed models, Yu and Van Aerde, and state-of-art Robertson formulation. Figure 10 demonstrates the downstream flow profile for the proposed model-1 (which produced the least error among all the proposed models) and the Yu and Van Aerde formulation. As was the case for the field data analysis, the accuracy of Yu and Van Aerde formulation deteriorates as the time step increases, while the accuracy of the proposed models increases slightly, and the accuracy of the Robertson formulation remains almost constant, as demonstrated in Figure 11. The results of Figure 11 and Figure 8 clearly demonstrate the consistency between simulated and field-observed traffic dispersion behavior. Consequently, the study demonstrates the effectiveness of the INTEGRATION software for the modeling of platoon dispersion behavior.

CONCLUSIONS AND RECOMMENDATIONS FOR FURTHER RESEARCH

The paper demonstrates the importance of the Yu and Van Aerde calibration procedure for the commonly accepted Robertson platoon dispersion model, which is implemented in the TRANSYT-7F software. The paper demonstrates that the formulation results in an estimated downstream cyclic profile with a margin of error that increases as the size of the time step increases. In an attempt to address this shortcoming, the paper proposes the use of three enhanced geometric distribution formulations that explicitly account for the time-step size within the modeling process. The proposed models were validated against field and simulated data. The results clearly demonstrate that the proposed model prediction error is not affected by the size of the modeling step size. Furthermore, the study demonstrates that the modeling of traffic dispersion within the INTEGRATION software is consistent with field observations and thus can serve as a tool for testing various traffic dispersion models.

It is anticipated that the implementation of the proposed formulations can enhance the accuracy of traffic dispersion modeling that is key to the design of off-line and real-time traffic-signal control systems. Furthermore, the proposed models can be integrated within an Advanced Traveler Information System (ATIS) to enhance dynamic roadway travel time predictions.

As is the case with any research effort, it is recommended that further research be conducted. Specifically, a comprehensive sensitivity study is required in order to quantify the effect of various

roadway and traffic characteristics on traffic dispersion behavior. Second, it is recommended that additional field data be gathered and that simulated data be assembled in order to construct a comprehensive dataset for model validation purposes.

ACKNOWLEDGEMENTS

The authors would like to acknowledge the financial support of the Mid-Atlantic University Transportation Center (MAUTC) in conducting this research effort.

REFERENCES

- Guebert, A.A. and Sparks, G. Timing Plan Sensitivity to Changes in Platoon Setting, University of Saskatoon.
- Hall, M.D., Van Vliet, D., and Willumsen, L.G. SATURN – A Simulation/Assignment Model for the Evaluation of Traffic Management Schemes. *Traffic Engineering and Control*, Vol. 21, No. 4, 1980, pp. 168-176
- Hunt, P.B., Robertson, D.I., Bretherton, R.D. and Winton, R.I. *SCOOT – A Traffic Responsive Method of Coordinating Signals*. RRL Tool. RRL Report LR 1041, Road Research Laboratory, Crowthorne, Berkshire, U.K., 1981.
- Lieberman, E.B. and Andrews, B.J. TRAFLO – A New Tool to Evaluate Transportation Management Strategies. *Transportation Research Record 772*, TRB, National Research Council, Washington D.C., 1980, pp. 9-15.
- Manar, A. *Modelisation de la Dispersion du Trafic Entre les Carrefours*. PhD Dissertation at the Civil Engineering Department, Universite de Montréal, Montréal, Canada, 1994.
- Pacey, G.M. *The Progress of a Bunch of Vehicles released from a Traffic Signal*. RRL Research Note RN/2665/GMP, Road Research Laboratory, Crowthorne, Berkshire, U.K., 1956 (unpublished).
- Rakha H. and Crowther B., Comparison and Calibration of FRESIM and INTEGRATION Steady-state Car-following Behavior, *Transportation Research*, 37A, pp. 1-27, 2003.
- Rakha H. and Ahn K., The INTEGRATION Modeling Framework for Estimating Mobile Source Emissions. *Journal of Transportation Engineering*, In press.
- Robertson, D.I. *TRANSYT - A Traffic Network Study Tool*. RRL Report LR 253, Road Research Laboratory, Crowthorne, Berkshire, U.K., 1969.
- Seddon, P.A. Another Look at Platoon Dispersion: 2. The Diffusion Theory. *Traffic Engineering and Control*, 13(9), 1972a, pp. 388-390.
- Seddon, P.A. Another Look at Platoon Dispersion: 3. The Recurrence Relationship. *Traffic Engineering and Control*, 13(10), 1972b, pp. 442-444.
- Van Aerde M. Modeling of Traffic Flows, Assignment and Queuing in Integrated Freeway/Traffic Signal Networks, Ph.D. thesis, Department of Civil Engineering, University of Waterloo, Waterloo, Canada, 1985.
- Van Aerde M. and Yagar S., Dynamic Integrated Freeway/Traffic Signal Networks: Problems and Proposed Solutions, *Transportation Research*, Vol. 22A, No. 6, pp. 435-443, 1988a.
- Van Aerde M. and Yagar S. Dynamic Integrated Freeway/Traffic Signal Networks: A Routing-Based Modeling Approach, *Transportation Research*, Vol. 22A, No. 6, pp. 445-453, 1988b.

- Van Aerde M. and Rakha H. Multivariate Calibration of Single-Regime Speed-Flow-Density Relationships, *Vehicle Navigation and Information Conference (VNIS)*. IEEE, Piscataway NJ, USA 95CH35776, pp.334-341, 1995.
- Van Aerde, M. and Rakha. H.A. *INTEGRATION release 2.3 for windows: User's Guide*, Virginia Tech Transportation Institute, Blacksburg, Virginia, 2002.
- Wang, D., Zhang, Y. and Zhitao, W. Study of Platoon Dispersion Models. *Transportation Research Board Annual Meeting*, Washington D.C., 2003.
- Yu, L. and Van Aerde, M. Implementing TRANSYT's Macroscopic Platoon Dispersion in Microscopic Traffic Simulation Models. *Transportation Research Board Annual Meeting*, Washington D.C., 1995.
- Yu, L. and Van Aerde, M. Examination of Calibration of Platoon Dispersion Parameters Based on Link Travel Time Statistics. *Transportation Research Board Annual Meeting*, Washington D.C., 2000.

LIST OF TABLES

Table 1: Characteristics Used For Calibrating Different Platoon Dispersion Models

Table 2: Numerical Example of Proposed Model-1 for $n=4$ (s)

Table 3: Numerical Example of Proposed Model-2 for $n=4$ (s)

Table 4: Numerical Example of Proposed Model-3 for $n=4$ (s)

Table 5: Characteristics of Montréal Dataset

Table 6: Characteristics of Simulated Roadway

Table 7: Characteristics of Simulated Dataset

LIST OF FIGURES

Figure 1: Robertson Platoon Dispersion Model

Figure 2: Predicted Downstream Flow Profiles From Different Models

Figure 3: Upstream and Predicted Downstream Flow Profiles

Figure 4: Parametric Second-by-Second Platoon Dispersion Derivation

Figure 5: Field Test Site (Montréal, Canada - MapQuest.com, Inc)

Figure 6: Observed Upstream Flow Profile (Manar 1994)

Figure 7: Observed and Predicted Downstream Flow Profiles (Montréal Data)

Figure 8: Error in Predicted Downstream Flow Profile

Figure 9: Simulated Network Configuration

Figure 10: Observed and Predicted Downstream Flows

Figure 11: Error in Predicted Downstream Flow Profile

Table 1: Characteristics Used For Calibrating Different Platoon Dispersion Models

Model	Required Factors
Robertson's Model	$T_a = 20$ (sec) $\alpha = 0.25$ $\beta = 0.8$
Pacey's Model	$V_a = 36$ (km/h) $\sigma_v = 3.6$ (km/h)
Normal Distribution of Travel Time	$T_a = 20$ (sec) $\sigma_t = 3.464$ (sec)
Lognormal Distribution of Travel Time	$T_a = 20$ (sec) $\sigma_t = 3.464$ (sec)
Lognormal Distribution of Speed	$V_a = 36$ (km/h) $\sigma_v = 3.6$ (km/h)

Table 2: Numerical Solution of Model-1 (n=4s, F=0.111, T=32s)

				$w_k = F \cdot (1-F)^k \cdot \frac{n - i-n-k }{n}$										
t (s)	i	t-(T+i,n)	$q_{t-(T+i,n)}$ (veh/h/lane)	k=0	k=1	k=2	k=3	k=4	k=5	k=6	k=7	$\sum_k w_k$	$q'_{t,i}$ (veh/h/lane)	q'_t (veh/h/lane)
34	0	2	2000	0.111	0.074	0.044	0.020	-	-	-	-	0.249	497	497
38	0	6	1000	0.111	0.074	0.044	0.020	-	-	-	-	0.249	249	813
	1	2	2000	-	0.025	0.044	0.059	0.069	0.046	0.027	0.012	0.282	565	

Table 3: Numerical Solution of Model-2 (n=4s, F=0.111, T=32s)

				$w_k = F \cdot (1-F)^{k-1}$										
t (s)	i	t-(T+i,n)	$q_{t-(T+i,n)}$ (veh/h/lane)	k=0	k=1	k=2	k=3	k=4	k=5	k=6	k=7	$\sum_k w_k$	$q'_{t,i}$ (veh/h/lane)	q'_t (veh/h/lane)
34	0	2	2000	0.111	0.099	0.088	0.078	-	-	-	-	0.376	751	751
38	0	6	1000	0.111	0.099	0.088	0.078	-	-	-	-	0.376	376	845
	1	2	2000	-	-	-	-	0.069	0.062	0.055	0.049	0.235	469	

Table 4: Numerical Solution for Model-3 (n=4s, T=32s)

t (steps)	i	T (steps)	F_4	t-i	q_{t-i} (veh/h/lane)	$F(1-F)^{t-i}$	$q'_{t,i}$ (veh/h/lane)	q'_t (veh/h/lane)
9	8	8	0.373	1	2000	0.373	746	746
10	8	8	0.373	2	1000	0.373	373	841
	9	8	0.373	1	2000	0.234	468	

Table 5: Characteristics of Montréal Dataset

Dist. (m)	Step Size (s)	Travel Time (s)		Platoon Dispersion Factor - α					Travel-time factor - β				
		Mean	σ	Prop. Model 1	Prop. Model 2	Prop. Model 3	Yu & Van Aerde	Robertson	Prop. Model 1	Prop. Model 2	Prop. Model 3	Yu & Van Aerde	Robertson
200	2	19.00	7.60	0.59	0.59	0.54	0.59	0.23	0.63	0.63	0.65	0.63	0.8
	4					0.45					0.69		
	6					0.37					0.73		
300	2	30.50	11.3	0.54	0.54	0.52	0.54	0.25	0.65	0.65	0.66	0.65	0.8
	4					0.45					0.69		
	6					0.39					0.72		

Table 6: Characteristics of Simulated Roadway

Link Characteristic	Parameter
Roadway length (m)	300
Free-flow speed (km/h)	50
Speed-at-capacity (km/h)	35
Capacity (veh/h/lane)	1800
Jam density (veh/km/lane)	100
Number of lanes	3
Number of loop detectors	3
Speed coefficient of variation (percent)	10
Entering headway distribution	100% Random (Exponential Distribution)
Total Simulation Time (s)	600

Table 7: Characteristics of Simulated Dataset

Dist. (m)	Step Size (s)	Travel Time (s)		Platoon Dispersion Factor - α					Travel-time factor - β				
		Mean	σ	Prop. Model 1	Prop. Model 2	Prop. Model 3	Yu & Van Aerde	Robertson	Prop. Model 1	Prop. Model 2	Prop. Model 3	Yu & Van Aerde	Robertson
200	2	17.38	1.59	0.08	0.08	0.05	0.08	0.27	0.93	0.93	0.95	0.93	0.8
	6					0.02					0.98		
300	2	25.44	2.29	0.08	0.08	0.06	0.08	0.32	0.93	0.93	0.94	0.93	0.8
	6					0.03					0.97		

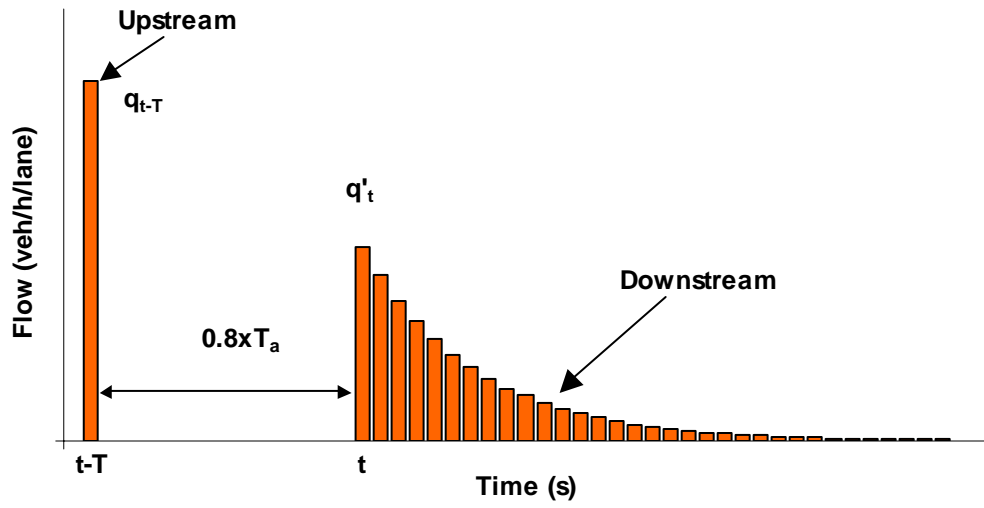


Figure 1: Robertson Platoon Dispersion Model

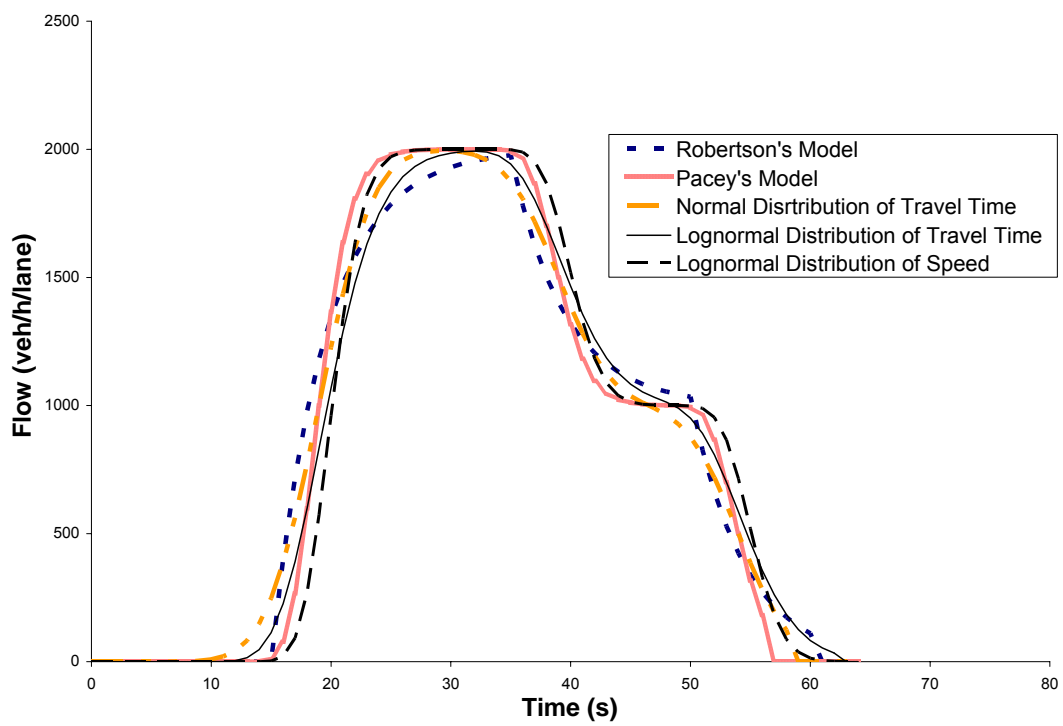


Figure 2: Predicted Downstream Flow Profiles From Different Models

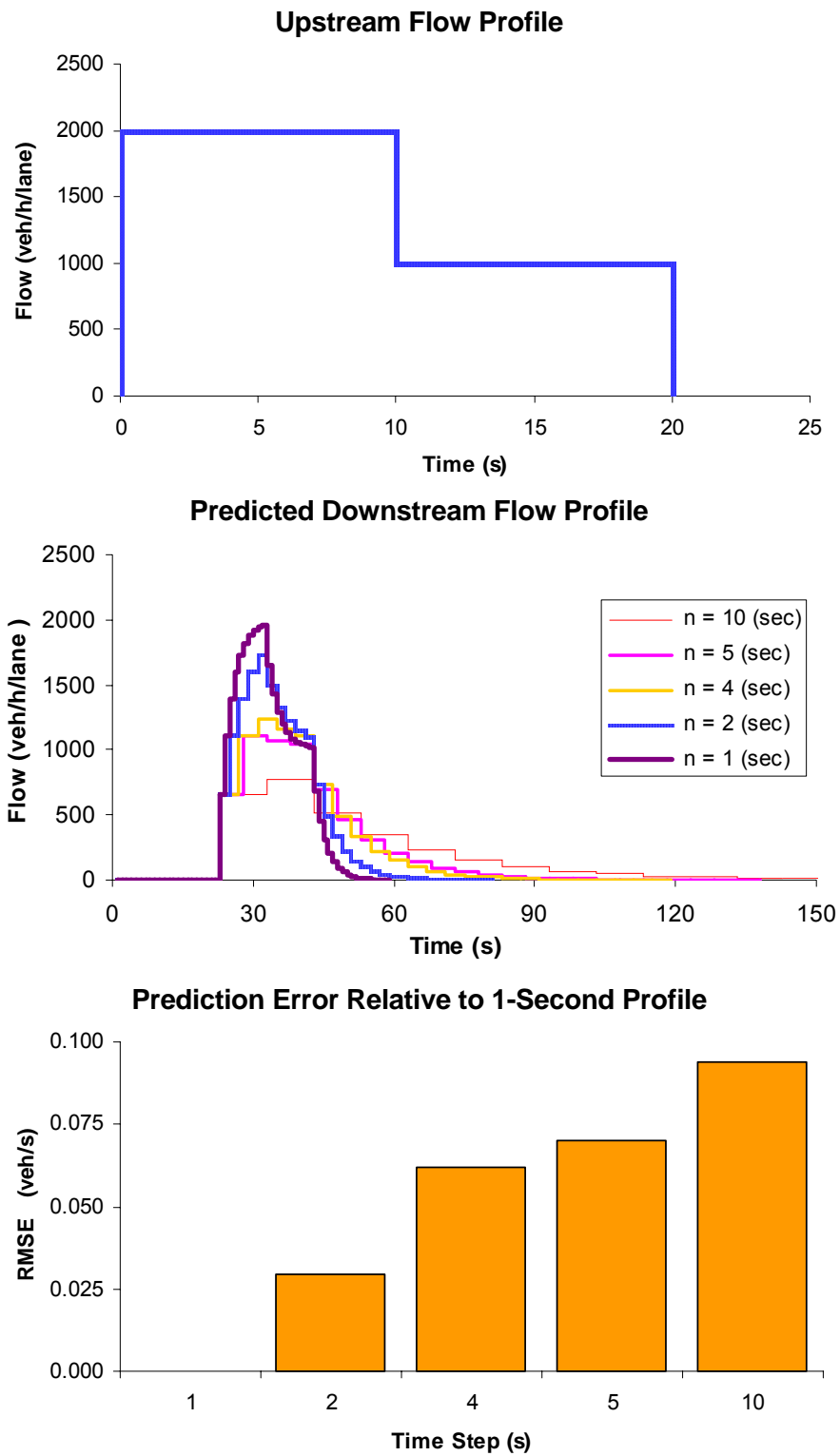


Figure 3: Upstream and Predicted Downstream Flow Profiles

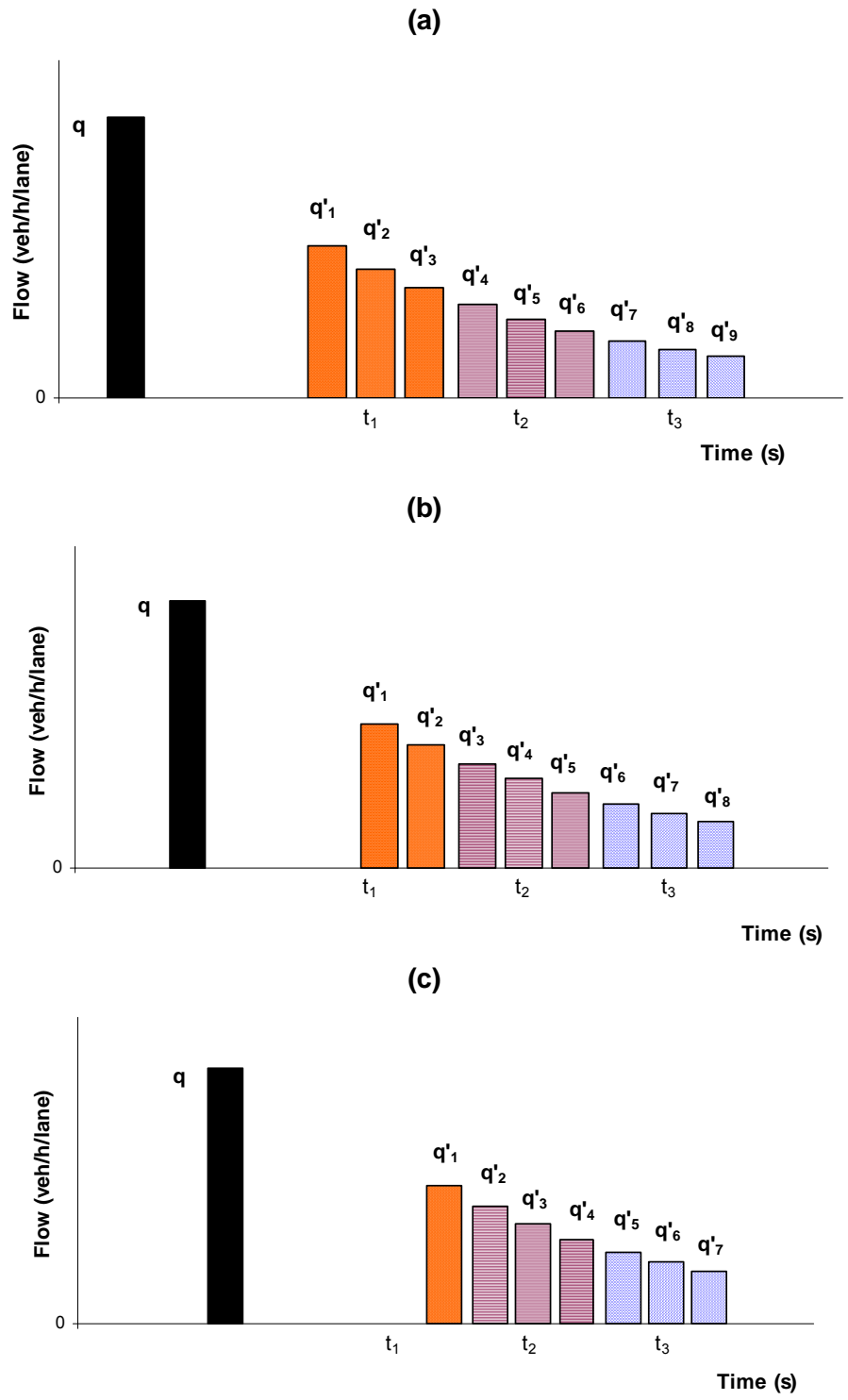


Figure 4: Parametric Second-by-Second Platoon Dispersion Derivation

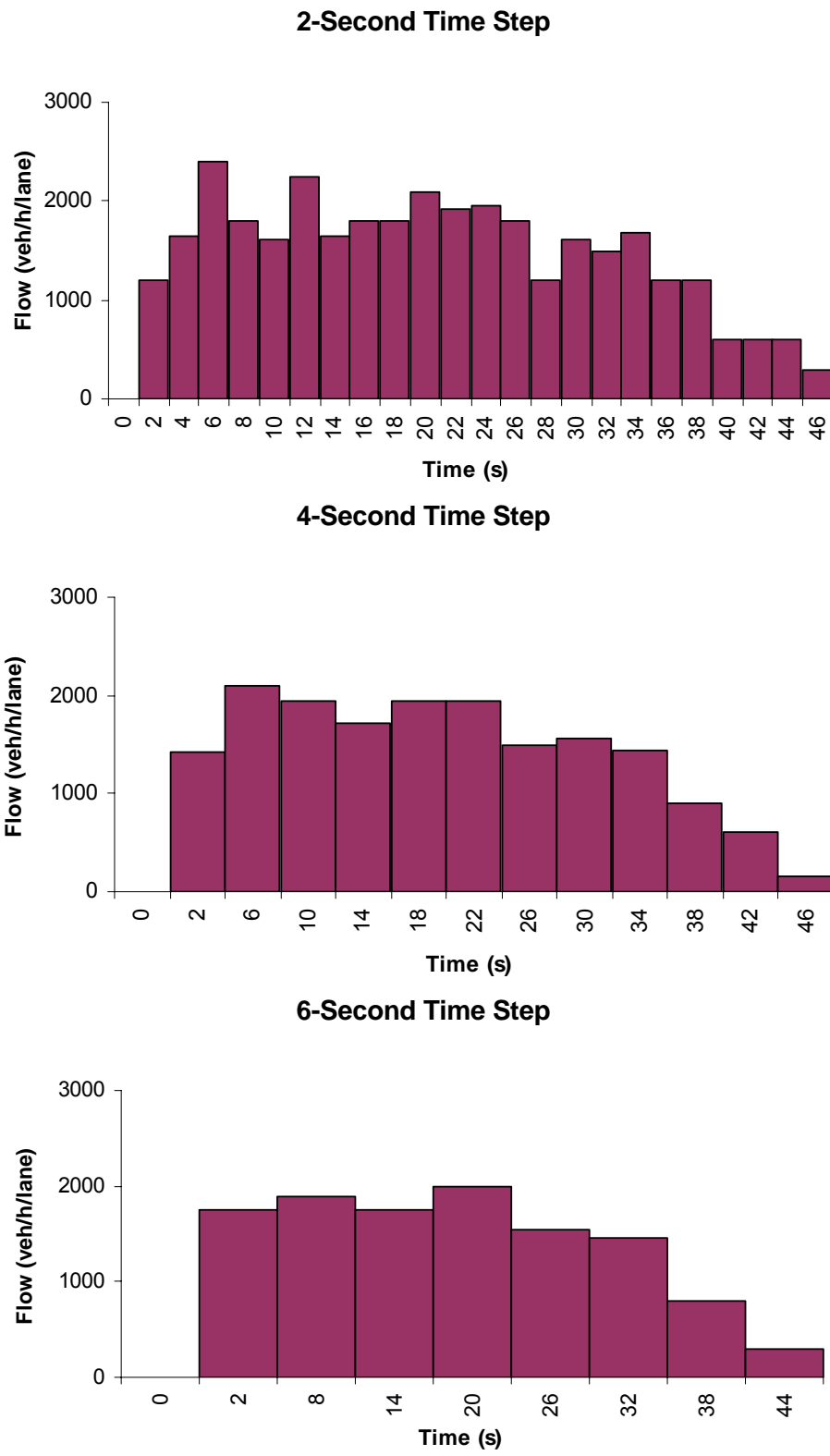


Figure 6: Observed Upstream Flow Profile (Manar 1994)

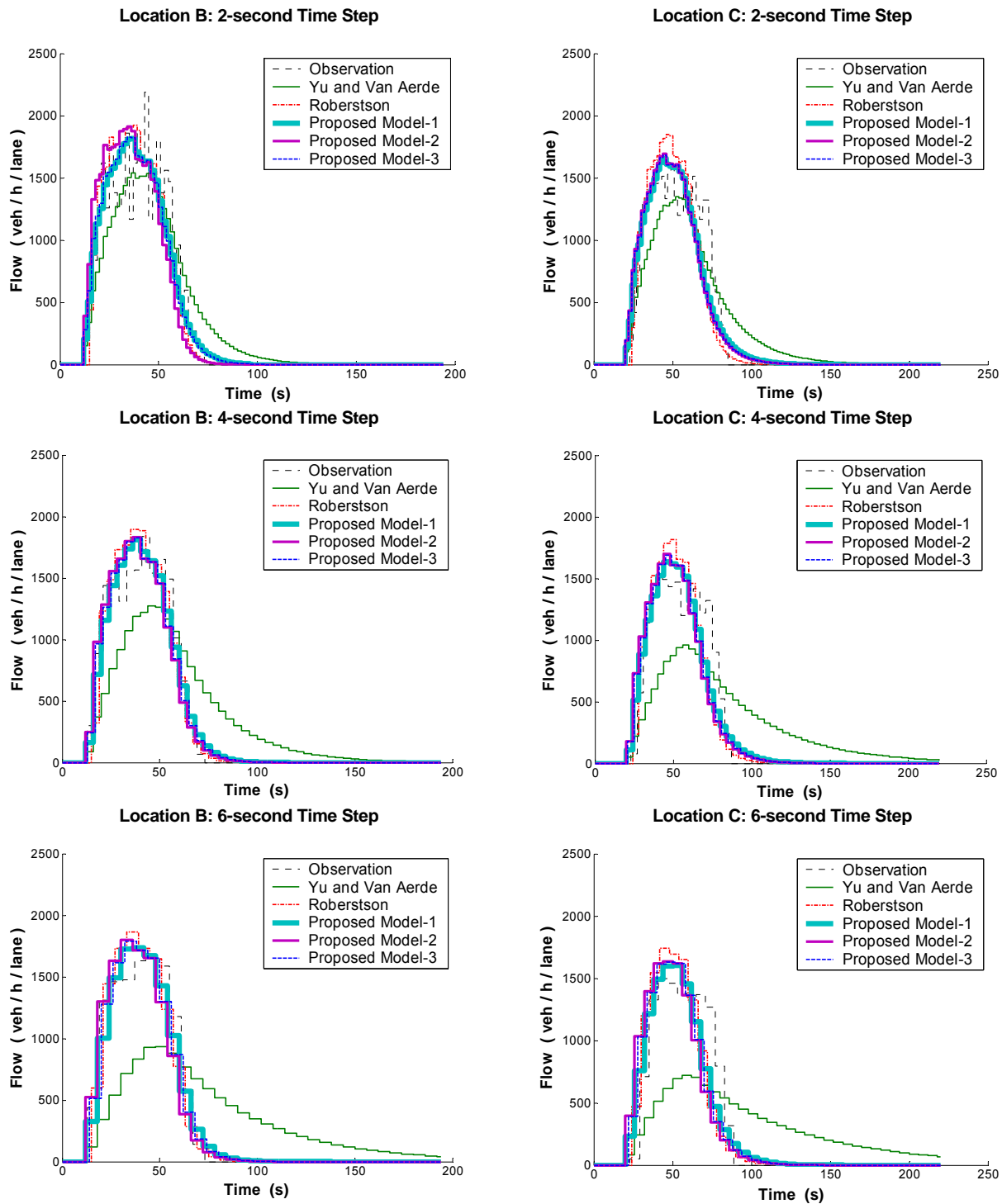


Figure 7: Observed and Predicted Downstream Flow Profiles (Montréal Data)

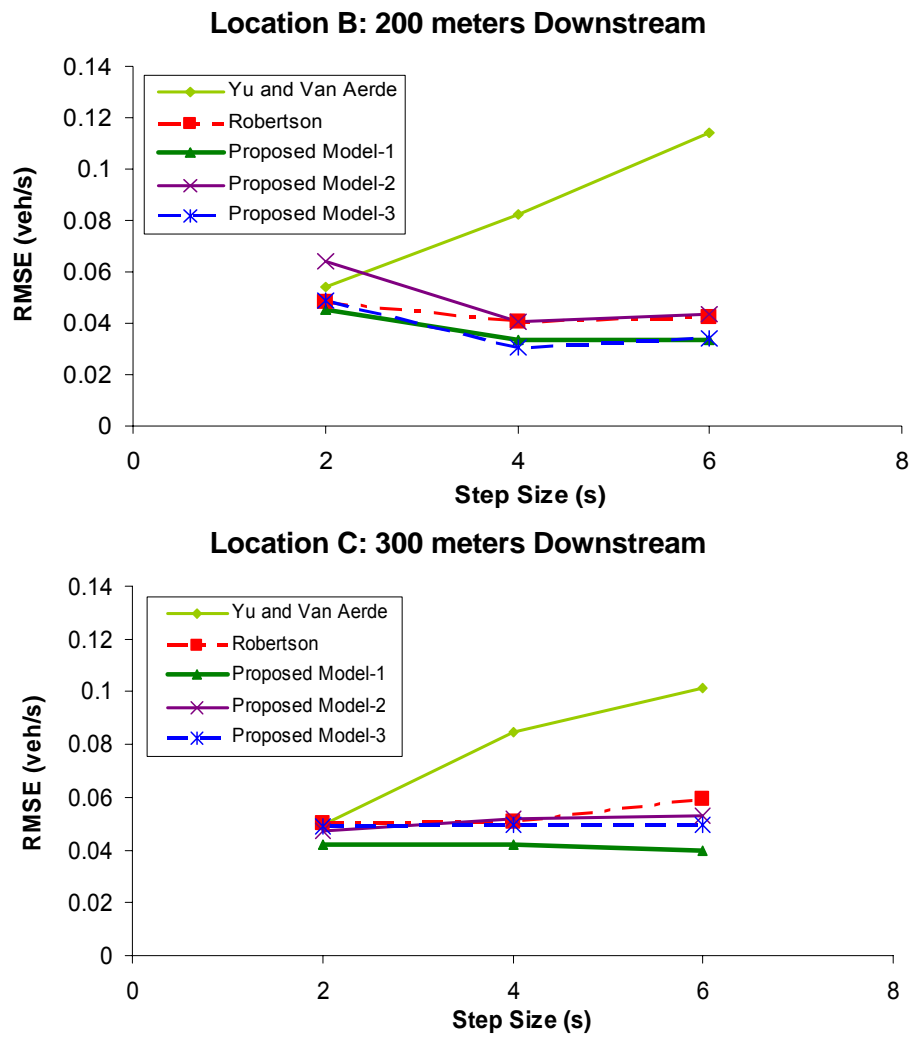


Figure 8: Error in Predicted Downstream Flow Profile

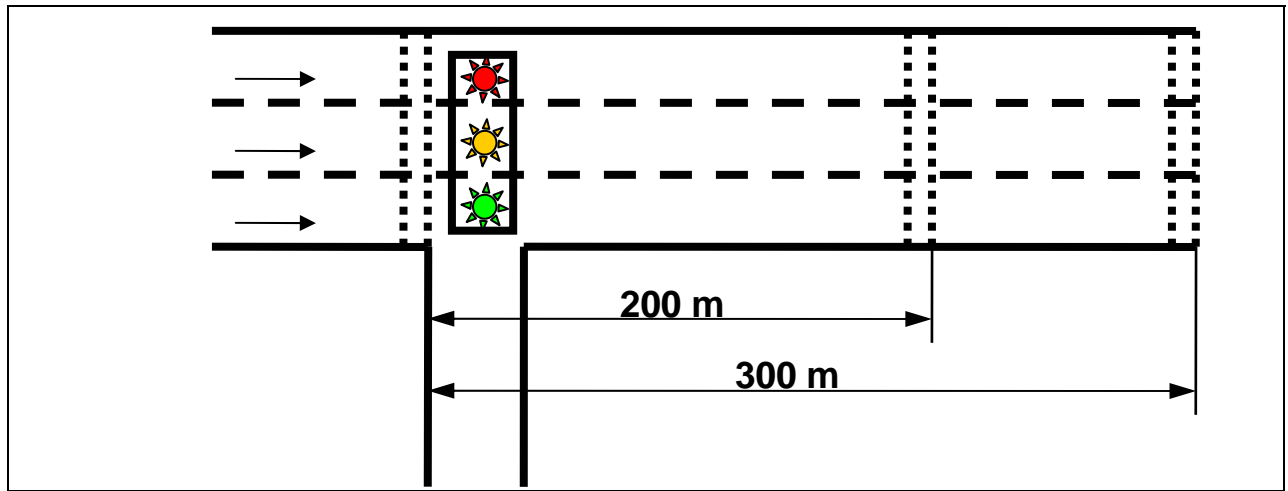


Figure 9: Simulated Network Configuration

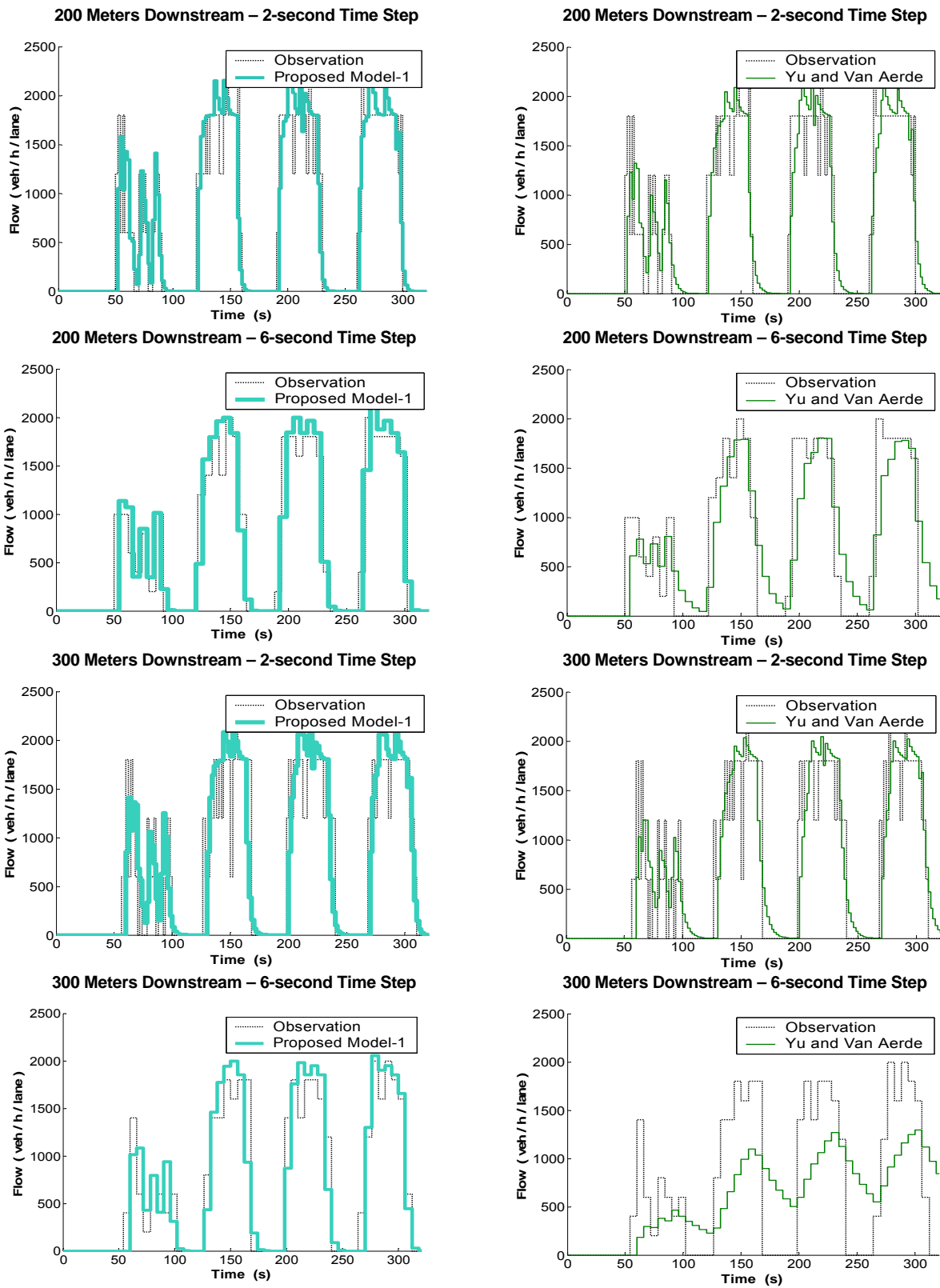


Figure 10: Observed and Predicted Downstream Flows

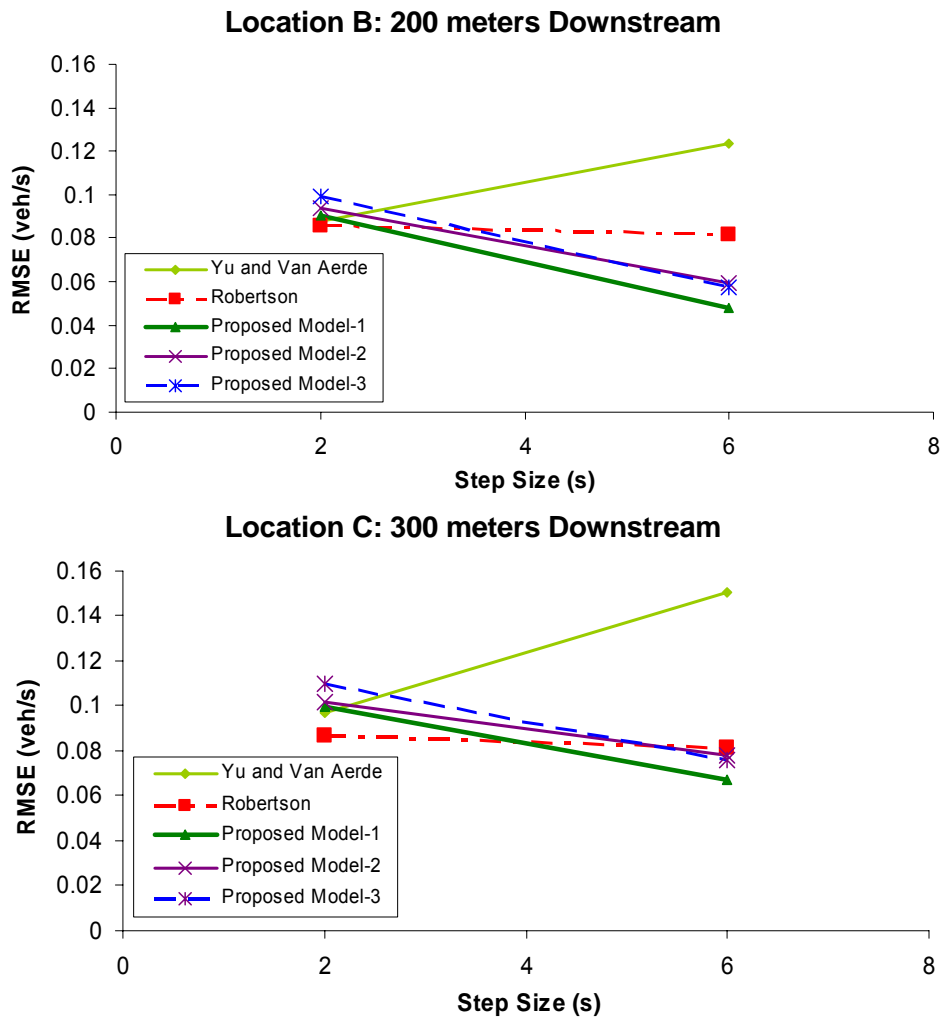


Figure 11: Error in Predicted Downstream Flow Profile

APPENDIX A

CALIBRATION OF PLATOON DISPERSION FACTOR AND TRAVEL-TIME FACTOR

The recurrence platoon dispersion equation in TRANSYT was derived by Seddon (1972) as,

$$q'_t = \sum_{i=T}^{\infty} F \cdot (1-F)^{i-T} \cdot q_{t-i} \quad [\text{A.1}]$$

$$F = \frac{1}{1 + \alpha \cdot \beta \cdot T_a} \quad [\text{A.2}]$$

Where:

q'_t : arrival flow at the downstream intersection at time t (veh/h);

q_t : departure flow at the upstream intersection at time t (veh/h);

T : minimum travel time on the roadway, equal to $\beta \cdot T_a$;

α : dimensionless platoon dispersion factor;

β : dimensionless travel-time factor;

F : dimensionless smoothing factor, and

T_a : mean roadway travel time (s).

The function within equation A.1 is computed as

$$P_r(X = i) = F(1-F)^{i-T} \quad (i = T, T + 1, \dots) \quad [\text{A.3}]$$

is a probability function. Travel time i in A.3 follows a shifted geometric distribution, because the geometric distribution takes the form of

$$P_r(X = i) = F(1-F)^{i-1} \quad (i = 1, 2, \dots) \quad [\text{A.4}]$$

The population means of A.3 and A.4 are different, but their standard deviations are the same.

Under the assumption that the travel time follows the shifted geometric distribution and that the average travel time T_a and the standard deviation of travel time σ are given, one can calibrate α and β in terms of T_a and σ .

According to the definition of the geometric distribution and A.3, the expectation of the distribution is computed as,

$$E(i - T + 1) = \frac{1}{F} \quad [\text{A.5}]$$

Therefore,

$$(T_a - T + 1) = \frac{1}{F} \quad [\text{A.6}]$$

Substituting A.2 into A.6, one gets

$$(T_a - \beta \cdot T_a + 1) = 1 + \alpha \cdot \beta \cdot T_a \quad [\text{A.7}]$$

Equation A.7 can be solved to derive the relationship between α and β as

$$\beta = \frac{1}{\alpha + 1} \text{ or } \alpha = \frac{1 - \beta}{\beta} \quad [\text{A.8}]$$

Moreover, the standard deviation of $(i-T+1)$ in equation A.3 is the standard deviation of travel time and can be computed as

$$\frac{1-F}{F^2} = \sigma^2. \quad [\text{A.9}]$$

Substituting A.2 into A.9, one gets

$$\alpha \cdot \beta \cdot T_a (1 + \alpha \cdot \beta \cdot T_a) = \sigma^2. \quad [\text{A.10}]$$

Solving equation A.10 gives

$$\beta = \frac{2T_a + 1 \pm \sqrt{1 + 4\sigma^2}}{2T_a}. \quad [\text{A.11}]$$

From A.8, it can be said that $\alpha \geq 0$ and $\beta \leq 1$. Therefore,

$$\beta = \frac{2T_a + 1 - \sqrt{1 + 4\sigma^2}}{2T_a}. \quad [\text{A.12}]$$

Substituting A.12 into A.8, we get

$$\alpha = \frac{\sqrt{1 + 4\sigma^2} - 1}{2T_a + 1 - \sqrt{1 + 4\sigma^2}}. \quad [\text{A.13}]$$

From A.9, one gets

$$F = \frac{\sqrt{1 + 4\sigma^2} - 1}{2\sigma^2}. \quad [\text{A.14}]$$

Consequently, Equations A.12, A.13, and A.14 can be used to calibrate α and β or F from the mean and variance of travel times over the drive section.